JBUON 2013; 18(4): 996-1005
ISSN: 1107-0625, online ISSN: 2241-6293 • www.jbuon.com
E-mail: editorial_office@jbuon.com

ORIGINAL ARTICLE

# Proteomic studies of multiple myeloma in RPMI8226 cell line treated with bendamustine

Chenglong Sun*, Juan Li*, Jingli Gu, Junru Liu, Beihui Huang

*Department of Hematology, First Affiliated Hospital of Sun Yat-sen University, Guangzhou, 510080 China*
**Equal contributors in this study*

## Summary

***Purpose:*** *Multiple myeloma (MM) is a malignant and incurable neoplasm of plasma cells that accumulate in the bone marrow. Bendamustine, an antitumor agent including double property of alkylating agent and purine analogues, displayed clinical antitumor activity in patients with MM. However, the precise mechanism of action of bendamustine has not been completely elucidated.*

***Methods:*** *In this study, we established the cell model of bendamustine-induced MM RPMI8226 cell apoptosis, and used two dimensional differential in-gel electrophoresis (2D-DIGE) proteomics to analyze the bendamustine-induced protein alterations.*

***Results:*** *Our results revealed that compared with control group, bendamustine significantly inhibited the proliferation of RPMI8226 cells in a concentration-dependent and time-dependent manner. Proteomic approach was performed to identify 30 differentially expressed proteins in RPMI8226 cells upon bendamustine treatment, which included 15 up-regulated and 15 down-regulated proteins. Of these, protein disulfide isomerase A3 (PDIA3) and cytokine-induced apoptosis inhibitor 1 (CPIN1), were selected for further studies.*

***Conclusion:*** *These results implicate PDIA3 and CPIN1 as potential molecular targets for drug intervention in MM and thus provide novel insights into the mechanisms of antitumor activity of bendamustine.*

***Key words:*** *apoptosis, bendamustine, multiple myeloma, proteomics*

## Introduction

MM is a clonal B-cell malignancy characterized by aberrant expansion of plasma cells within the bone marrow and extramedullary sites and production of monoclonal immunoglobulin detectable in serum and/or urine. It accounts for approximately 1% of neoplastic diseases and 13% of hematologic cancers, seen as the most common cancer with skeleton as its primary site. Despite recent advances in stem-cell transplantation and chemotherapeutic drugs, the long-term survival rates remain poor and MM remains incurable an disease. Therefore, there is a need to develop new therapeutic strategies in order to improve the prognosis of patients with MM [1,2].

Bendamustine, as a unique alkylating agent and purine analogue, has shown distinctive clinical activity against various cancers. The agent was approved by the Food and Drug Administration (FDA) of the United States for the treatment of chronic lymphocytic leukemia (CLL) and indolent B-cell non-Hodgkin lymphoma (NHL) in 2008 [3,4]. At the same time, bendamustine has also been applied in the treatment of patients with MM, especially for relapsed or refractory cases. For patients with advanced MM, bendamustine is effective and associated with mild toxicity [5]. Bendamustine can induce DNA damage, weaken DNA repair, and interfere with cell karyokinesis by regulating the checkpoints to inhibit the proliferation of MM cells [6,7], but the detailed mechanism remains unknown. It is necessary to adopt more advanced experimental techniques to explore this topic.

*Correspondence to:* Juan Li, MD. Department of Hematology, First Affiliated Hospital of Sun Yat-sen University, Guangzhou, China.
Tel: +86 20 877 557 66-8831, Fax: +86 20 87333 455, E-mail: luliyuan@tom.com; myeloma_sysu@163.com
Received: 12/06/2013; Accepted: 13/07/2013

Proteomic techniques, as a powerful research tool, recently have played an important role in large-scale protein studies. With advances in technology, two 2D-DIGE has become one of the most effective methods for the separation, detection, and quantitation of proteins [8,9]. Proteomics offer important theoretical references for studying the mechanism of the disease and finding possible targets of drug action at the protein level.

In this study, we chose MM RPMI8226 cell line as our objective to establish the model of inducing apoptosis with bendamustine. Proteomics method was used to screen the protein which changed before and after drug treatment and the important protein related to apoptosis was then detected among these proteins. It was expected to find out the target of bendamustine action and its mechanism of inducing apoptosis in order to offer new in sights in treating MM.

## Methods

*Cell culture*

The human MM cell line RPMI8226 was obtained from the American Type Culture Collection (Rock-ville,MD,USA). RPMI8226 cells were cultured in RPMI 1640 medium (Gibco) supplemented with 10% heat-inactivated fetal bovine serum (Gibco), 100 U/mL penicillin (Gibco) and 100 mg/mL streptomycin (Gibco) in a humidified incubator containing 5% CO in air at 37°C. The cells were subcultured every 23 days, and all experiments were carried out using the log phase cells. Bendamustine was dissolved in dimethylsulfoxide (DMSO; Sigma-Aldrich).

*Reagents and antibodies*

Bendamustine, propidium iodide (PI) and methyl thiazolyltetrazolium (MTT) were purchased from Sigma-Aldrich (St Louis, MI, USA). Annexin-V assay kit was obtained from Life Technologies Corporation (Grand Island, NY, USA). Anti-cleaved caspase-3, and caspase-3 antibodies were purchased from BD Biosciences (San Jose, California, USA) and protein disulfide isomerase A3 (PDIA3) and cytokine-induced apoptosis inhibitor 1 (CPIN1) monoclonal antibodies were purchased from Santa Cruz Biotechnology (Santa Cruz, CA, USA). The horseradish peroxidase-conjugated secondary antibody and anti-GAPDH antibody were purchased from Protein Tech Group (Chicago, IL, USA) All reagents for performing 2D-DIGE, including CyDye DIGE fluor dye Cy2, Cy3 and Cy5, dithiothreitol (DTT), Iodoacetamide (IAA), 3-[(3-cholamidopropyl)-dimethylammonio]-1-propane sulfonate (CHAPS), pH gradient Immobiline DryStrip, 2-D Clean-up kit and 2-D Quant kit, were purchased from GE Healthcare (Piscataway, NJ, USA).

*Assay for cell proliferation inhibition (MTT assay)*

Cells were subcultured in a 96-well plate at a concentration of $1 \times 10^5$/mL (200 µl/well) and treated with 0, 5, 10, 25, 50 100 and 200 µg/ml of bendamustine for 24, 48 and 72 h, respectively. Subsequently, Twenty microlitre of phosphate buffered saline (PBS) solution containing 5 mg/mL MTT were added to each well, and cells were continuously incubated for an additional 4 h at 37˚C. After a brief centrifugation, supernatants were carefully removed and 150 µl DMSO were added to the cells. After insoluble crystals were completely dissolved, the absorbance of each sample was measured at 490 nm with a microtiter plate reader and optical density (OD) value was obtained to determine viable cells. The rate of cell proliferation was calculated by the following formula: cell proliferation rate = (A value in test group – A value in normal control group)/A value in normal control group × 100%. The values of half-maximal inhibitory concentration (IC50) of bendamustine at respective times were calculated using linear regression.

*Assessment of apoptosis on RPMI8226 cells by Annexin-V/PI double-staining assay*

After treatment with 100 µg/ml bendamustine at different hours, $1 \times 10^5$/mL RPMI8226 cells were collected and washed in cold PBS. Cells were stained with FITC-conjugated annexin V and propidium iodide (PI) by using the Annexin-V–FITC Apoptosis Detection kit (Invitrogen, USA) according to the instructions of the manufacturer. Apoptotic data acquisition and analysis were performed with use of FACSCalibur flow cytometer (Becton Dickinson, USA).

*Western blot analysis*

From the control and treatment groups, logarithmically growing cells were collected and homogenized with cell lysis buffer (20 mM Tris: pH 7.5, 150 mM NaCl, 0.25% NP40, 2.5 mM sodium pyprophosphate, 1 mM EGTA, 1 mM EDTA, 1 mM β-glycerophosphate,1 mM PMSF, 1 mM Na3VO4, 1 µg/ml leupeptin). The lysates were then incubated on ice for 30 min and centrifuged at 12000 rpm for 30 min. Protein concentrations were measured using the Bradford assay. The equal amounts of protein (50 µg) were subjected to 12% sodium dodecyl sulfate polyacrylamide gel electropheresis (SDS-PAGE) and electro-transferred onto nitrocellulose filters. The membranes were blocked with 5% non-fat dry milk for 1 h at room temperature and sliced according to the pre-stained molecular weight markers. The membranes were treated with primary antibodies: caspase-3 (1:1,000), cleaved caspase-3 (1:1,000), CPIN1 (1:1,000), PDIA3 (1:1,000) and GAPDH (1:1,000) , overnight at 4°C. The membranes were washed three times for 10 min each with Tris-Tween Buffered Saline (PBS containing 0.05% Tween 20), and then incubated in horseradish peroxidase-conjugated secondary antibody

for 2 h at room temperature. The protein bands were detected with an enhanced chemiluminescence kit and the ECL system, according to the manufacturer's instructions.

*2D-DIGE*

*Protein preparation and protein labeling*

After a 12-h treatment with 100 μg/ml bendamustine and PBS, the RPMI8226 cells ($2 \times 10^6$ cells/100-mm dish) were washed three times in PBS and then resuspended in 400 μl of 2D-DIGE lysis buffer (7M urea, 2 M thiourea, 4% (w/v) CHAPS, 40 mM Tris base, 5 mM magnesium acetate, pH 8.5). The lysates were centrifuged at 12,000 rpm for 30 min at 4°C, and a part of them was used as source of protein for the next Western blot analysis. The other part was processed with 2-D Clean-up kit. After centrifugation, the pellets were resuspended with solution containing 7 M urea, 2 M thiourea and 4% CHAPS (w/v), and the pH was adjusted to 8.5. Protein concentrations were determined using 2-D Quant Kit according to operations guide, and the samples were stored at -80°C. The fluorescent dyes labeling for 2D-DIGE experiments was done as suggested by the manufacturer (GE Healthcare). In brief, 50 μg of protein sample from the control and treatment groups were labeled with 200 pmol of Cy3 or Cy5 dyes for comparison on the same gel. In order to avoid any possible deviations introduced by labeling efficiency, the samples of each group were alternatively labeled with both Cy3 and Cy5 dyes. The labelling reactions were performed for 30 min on ice in the dark and then quenched by 10 mm lysine for 10 min on ice. A pooled sample consisting of equal amounts of all samples (both control and treatment groups) was used as the pooled internal standard and labeled with Cy2, and it was used as a standard on all gels to facilitate image matching and cross-gel statistical analysis. Three independent biological technical duplicates were done in this study.

*2D -DIGE*

The 2-dimension electrophoresis was carried out using GE Healthcare reagents and equipment. According to the results of preliminary experiments, 24 cm pH4 -7 IPG strips were selected for first dimension isoelectric focusing separation. The strips were incubated overnight in 450 μl of rehydration buffer (7 M urea, 2 M thiourea, 4% (w/v) CHAPS, 40 mM DTT, 1% IPG buffer (pH 4–7), 0.002% (w/v) Bromophenol blue). The labeled protein mixture of each gel was applied on a 130 mm × 3 mm × 0.5 mm immobilized DryStrip strips. Isoelectric focusing (IEF) was performed using the following condition by Ettan IPGphor II IEF system: 12 h at 30 V, 1 h at 500 V, 1 h at 1000 V, 10 h at 8000 V and a total of 81860 Vh. After IEF, the IPG strips were first equilibrated for 15 min with the equilibration buffer containing 6 M urea, 30%(w/v) glycerol, 2% (w/v) SDS, and 50 mM Tris, pH 8.8 ,0.002% (w/v) bromophenol blue and 1% (w/v) DTT, and then equilibrated for 15 min with the similar buffer containing 2.5% (w/v) IAA instead of 1% (w/v) DTT. After equilibration, the strips were placed onto vertical 12.5% SDS-polyacrylamide gels in low fluorescence glass plates and sealed with 0.5% low melting point agarose for the second dimensional separation. Electrophoresis was run at 2 watts/gel for 30 min and then at 16 watts/gel until bromophenol blue completely reached the bottom of the gel at 20 °C with an Ettan-DALT six system.

*Image acquisition and data analysis*

All of the 2-DE gels were scanned directly using Typhoon 9400 fluorescence scanner (GE Healthcare) to produce gel images at the suitable excitation and emission different wavelengths from the Cy2, Cy3 and Cy5 labelled samples. Spot detection and matching were performed using ImageQuant software and the DeCyder 2D Software tool (GE Healthcare). The gels were poststained using Deep Purple, and the Biological Variation Analysis (BVA) module of Decyder Software was used to compare the treatment groups with control groups to search for the different expression of the proteins. For statistical purposes, the ratios of protein abundance that increased or decreased more than 1.5-fold with t-test score <0.05 were considered to be significant changes. The pick list of differentially expressed proteins was generated and exported into the Ettan Spot Picker (GE Healthcare). The matched protein spots were cut out for subsequent mass spectrometry (MS) analysis, while unmatched spots were deserted.

*Protein identification by mass spectrometry*

After transferred to Eppendorf tubes, spots were rinsed in MilliQ water for 10 min and hydrated with a decolorization solution of 25 mM $NH_4HCO_3$ in 50% (v/v) acetonitrile (ACN) 30 min at room temperature. The gel pieces were dried in a SpeedVac. This step was repeated three times until the gel pieces were destained. The spots were swollen overnight in a digestion buffer (12.5 ng/ml trypsin in 0.1 mol/L $NH_4HCO_3$). The resulting peptides were extracted out of the gel pieces three times with 50% ACN and 0.1% TFA. The digested protein was separated and identified by a Finnigan LTQ mass spectrometer. After digestion, the peptides were mixed in 0.5 μl of a 3 mg/ml solution of α-cyano-4-hydroxy-trans-cinnamic acid matrix in 0.1% TFA and 50% ACN, spotted onto the matrix-assisted laser desorption ionization (MALDI) target plate, and allowed to air dry. Matrix-assisted laser desorption ionization-time of flight (MALDI-TOF/TOF) mass spectrometer analyses was performed on an UltraFlex III (Bruker Daltonics) instrument according to the manufacturer's instructions. The peptide mass fingerprints (PMF) were acquired using the mass spectrometer in reflector mode.

Proteins were identified using MASCOT search engine software to match the spectra to a Swiss-Prot database. The identified proteins with Mowse scores of greater than 56 were considered significant ($p < 0.05$).

*Statistics*

All values given in this experiment were expressed as mean ± SD and analyzed using SPSS 17.0 software (SPSS Inc, Chicago, Illinois, USA). Statistical differences between the two groups were analyzed by Student's t-test. Statistical comparison of three or more groups and parameters were performed with one-way analysis of variance (ANOVA). Differences between two means with $p<0.05$ were considered statistically significant and $p<0.01$ very significant.

## Results

*Bendamustine inhibited the proliferation of RPMI8226 cells*

MTT assay was used to detect the effect of bendamustine on RPMI8226 cell proliferation. There was a dose-dependent and time-dependent manner inhibition of RPMI8226 cell proliferation by bendamustine (Figure 1). The results documented that bendamustine could significantly inhibit RPMI8226 cell proliferation *in vitro*. According to IC50 values of MTT assay, 100 μg/ml of bendamustine concentration were used in subsequent experiments. The IC50 value for growth inhibition at 48 h was 87.6 μg/ml and at 72 h it was 56.2 μg/ml. Therefore, 100 μmol/L bendamustine were used in subsequent experiments.

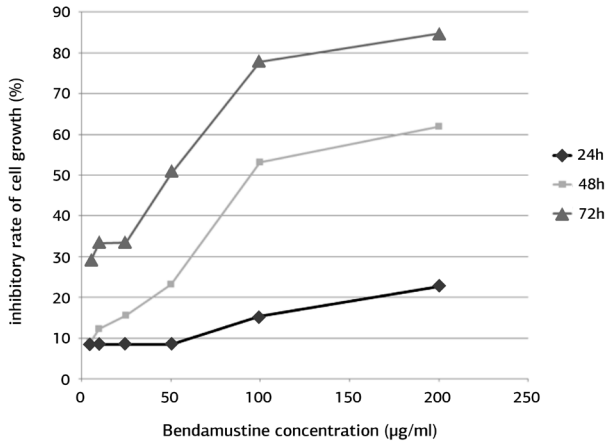


**Figure 1.** The effect of bendamustine on the proliferation of RPMI8226 cells by MTT assay. RPMI8226 cells were treated with 0, 5, 10, 25, 50, 100 and 200 μg/ml of bendamustine for 24, 48 and 72 h. Statistically significant differences were calculated between groups treated with different bendamustine concentrations at each time point and between different time points at each concentration ($p< 0.05$).

To evaluate whether RPMI8226 cell growth inhibition induced by bendamustine was the result of apoptosis or not, we initially performed flow cytometry to determine apoptosis in RPMI8226 cells exposed to 100 μg/ml of bendamustine concentration for 0, 2, 4, 8, 12 or 24 h. Annexin V (+) and PI (-) cells were considered early apoptotic cells, and Annexin V (+) and PI (+) cells were considered late apoptotic cells. As shown in Figure 2, the result indicated that the rate of cell apoptosis increased gradually in a time-dependent manner. At the same time, we used western blotting technique to detect changes about caspase-3 and cleaved caspase-3 protein expression in 100 μg/ml bendamustine-treated RPMI8226 cells at different time points. Caspase-3 and cleaved caspase-3

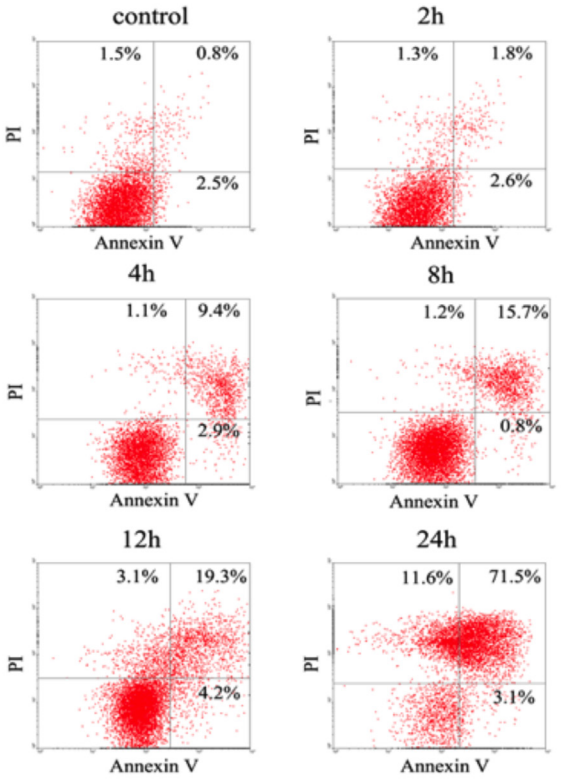


**Figure 2.** Apoptosis of RPMI8226 cells induced by bendamustine with flow cytometry. RPMI8226 cells were treated with 100 μg/ml bendamustine for 0, 2, 4, 8, 12 or 24 h, and apoptotic cells were detected by Annexin V/PI staining. The Annexin V positive portion represented the apoptotic fraction containing early and late apoptotic cells. The Figure shows the percentage of apoptotic RPMI8226 cells at different time points of bendamustine administration. Comparison of cell apoptosis between treatment group and control group at each time point showed, statistically significant difference ($p <0.05$).

protein were considered to play a central role in the execution-phase of cell apoptosis. The result indicated the prototype of the caspase-3 protein was cut over time after treatment, and we also showed a time-dependent increase in the levels of cleaved caspase-3 protein in bendamustine-treated cells (Figure 3). In short, both flow cytometry and western blotting analysis demonstrated that 100 μg/ml bendamustine induced RPMI8226 cell apoptosis in a time-dependent manner.

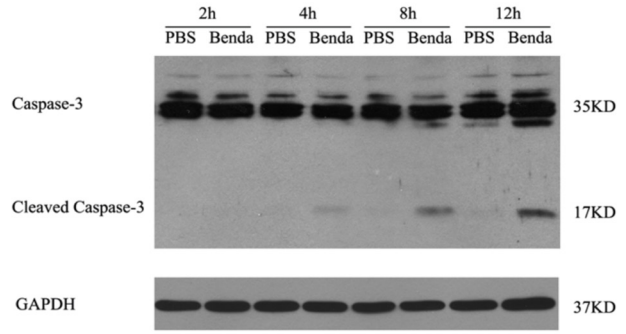


**Figure 3.** Effects of bendamustine on the expression of caspase-3 and cleaved caspase-3 in RPMI8226 cells. RPMI8226 cells were treated with 100 μg/ml bendamustine for 2, 4, 8, or 12 h. Cells were harvested, total proteins were extracted and immunoblotted for caspase-3 and cleaved caspase-3.Untreated RPMI8226 cells were used as controls. GAPDH was used as loading control

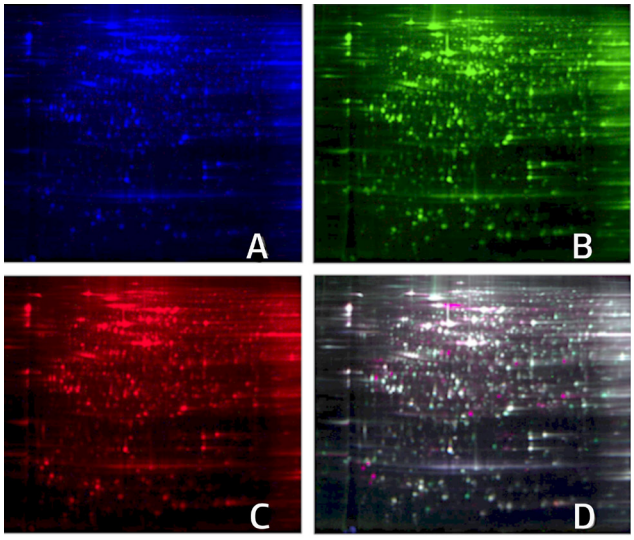


**Figure 4.** Image of 2D-DIGE analytical gels: **(A)**: 50 mg of Cy2-labeled internal standard (equal amount of normal and bendamustine-treated samples); **(B)**: 50 mg of Cy3-labeled normal samples; **(C)**: 50 mg of Cy5-labeled bendamustine-treated samples; **(D)**: color overlay of 2D-DIGE images of internal standard, normal and bendamustine-treated samples labeled with Cy2, Cy3 and Cy5.

*Proteomic results of 2D-DIGE patterns of RPMI8226 cells proteins treated with bendamustine*

To detect and evaluate the change of proteins expression in the RPMI8226 cell apoptotic model treated with 100 μg/ml bendamustine, 2D-DIGE analysis was performed. In order to prevent excessive protein degradation and modification changes, we selected 12 h as the appropriate point of treatment time for 2D-DIGE. RPMI8226 cells were exposed for 12 h with 100 μg/ml bendamustine (treatment group) or PBS (control group) respectively. The 2D-DIGE experiment was repeated three times. As shown in Figure 4, the blue image represented the internal standard labeled with Cy2 (Figure 4A). On the other hand, the green spots on the gel indicated the proteins in the control group (Figure 4B). Analogously, the red spots showed the protein in the treatment group (Figure 4C). All of the preceding images were overlapped to form a new fluorescent image (Figure 4D).

The gels were stained using Deep Purple Total Protein Stain, and protein spots were excised from the gel with an automated Spot Picker tool . In this study, we principally focused on two spots PDIA3 and CPIN1 the expression of which altered between treatment and control groups (Figure 5).

In order to search differentially expressed protein spots, the DIGE images were analyzed with Decyder Software. We selected the suitable protein meeting the following criteria protein expression change of at least 1.5-fold compared to the control group, appearance in at least three gels simultaneously and a significant statistical difference ($p<0.05$). Finally, we obtained a total of

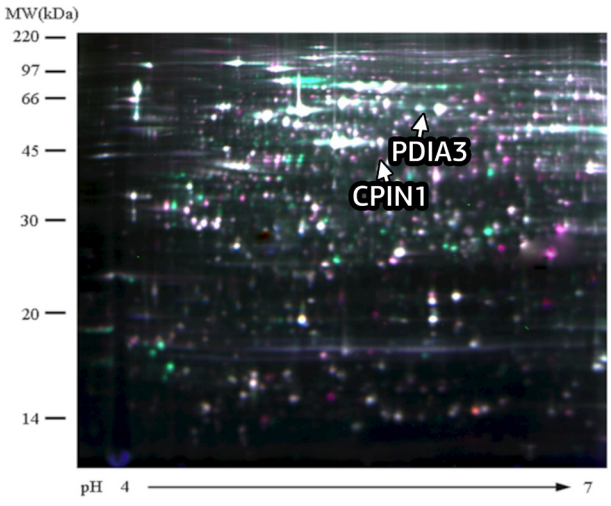


**Figure 5.** Image of 2D-DIGE analytical gels for PDIA3 and CPIN1.

76 differentially expressed protein spots. Three-dimensional and curve trend simulation graphs of the two proteins are shown in Figure 6 and 7.

According to the methodology described in Methods, MALDI-TOF/TOF mass spectrometer analyses were performed to obtain 76 protein spots PMF map. Proteins were identified by retrieving the SWISS-PROT database and the identified proteins' score in the database should be higher than 56 ($p<0.05$). Because some protein spots actually represent the same protein, a total of 30 proteins were finally identified. The results in Table 1 provide a list of identified proteins with their respective accession number, protein name, theoretical isoelectric point (PI), molecular weight (MW), the percentage of sequence coverage and average volume ratio. The average volume ratio of proteins represented the value of the treatment group compared to the control group. The PMF maps of PDIA3 and CPIN1 are displayed on Figure 8.

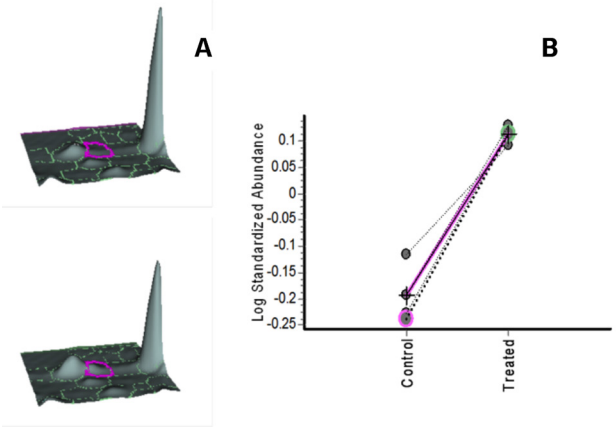


**Figure 6.** Simulating graph about the PDIA3 protein abundance of three-dimensional and curve trend. **(A)**: PDIS3 protein expression of the control and treatment groups, respectively. **(B)**: straight-line diagram of the protein changes.




**Figure 8.** The peptide mass fingerprints (PMF) maps of PDIA3 **(A)** and CPIN1 **(B)** are shown. The x-axis and y-axis represent the mass-to-charge ratio and the relative abundance of the identified protein respectively.

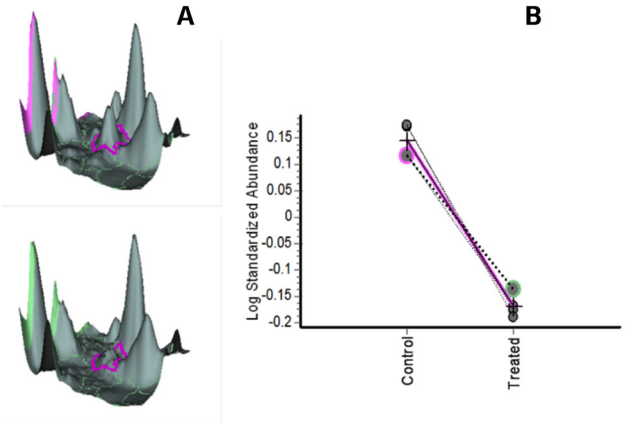


**Figure 7.** Simulating graph about the CPIN1protein abundance of three-dimensional and curve trend. **(A)**: CPIN1 protein expression of the control and treatment group, respectively. **(B)**: straight-line diagram of the protein changes.

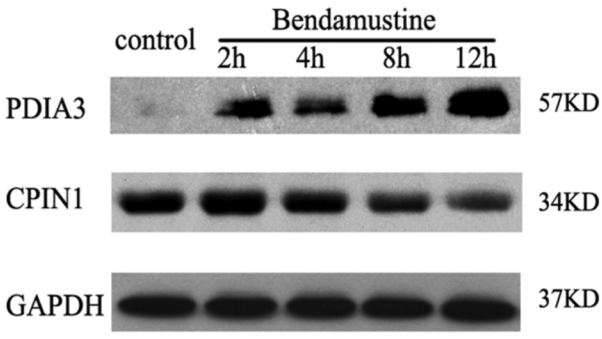


**Figure 9.** Western blot shows the changes of the expression level of PDIA3 and CPIN1 treated with bendamustine at different time points. GAPDH was used as internal control.

**Table 1.** Identities of differentially expressed proteins by MALDI-TOF-MS. Accession numbers of proteins were derived from SWISS-PROT database

| *Protein name* | *Accession number* | *MW (Da)* | *PI* | *Sequence coverage (%)* | *Volume ratio* |
|---|---|---|---|---|---|
| HSP74 Heat shock 70 kDa protein 4 | P34932 | 71082 | 5.11 | 26 | 2.09 |
| HS90B Heat shock protein HSP 90-beta | P08238 | 83554 | 4.97 | 39 | 19.34 |
| CH60 60 kDa heat shock protein, mitochondrial | P10809 | 61016 | 5.70 | 7 | -2.38 |
| VIM Vimentin | P08670 | 53676 | 5.06 | 56 | -2.07 |
| PDIA3 Protein disulfide-isomerase A3 | P30101 | 57146 | 5.98 | 18 | 2.02 |
| LMNB1 Lamin-B1 | P20700 | 66653 | 5.11 | 27 | 4.9 |
| HNRPK Heterogeneous nuclear ribonucleoprotein K | P61978 | 51230 | 5.39 | 26 | -2.23 |
| HNRPC Heterogeneous nuclear ribonucleoproteins C1/C2 | P07910 | 33707 | 4.95 | 34 | -2.31 |
| TCPA T-complex protein 1 subunit alpha | P17987 | 60819 | 5.8 | 27 | 2.13 |
| ACTA Actin, aortic smooth muscle | P62736 | 41982 | 5.23 | 4 | 4.32 |
| ACTB Actin, cytoplasmic 1 | P60709 | 42052 | 5.29 | 34 | 2.29 |
| CPIN1 Anamorsin,cytokine-induced apoptosis inhibitor 1 | Q6FI81 | 34131 | 5.44 | 30 | -2.05 |
| GLRX3 Glutaredoxin-3 | O76003 | 37693 | 5.31 | 32 | -2.04 |
| PP2AA Serine/threonine-protein phosphatase 2A catalytic subunit alpha isoform | P67775 | 36142 | 5.3 | 28 | 2.22 |
| ARMX1 Armadillo repeat-containing X-linked protein 1 | Q9P291 | 49720 | 9.32 | 13 | 6.47 |
| PRPS2 Ribose-phosphate pyrophosphokinase 2 | P11908 | 35146 | 6.15 | 27 | -5.25 |
| PSA3 Proteasome subunit alpha type-3 | P25788 | 28643 | 5.19 | 21 | -2.16 |
| PRDX6 Peroxiredoxin-6 | P30041 | 25133 | 6 | 58 | -3.42 |
| PRDX3 Thioredoxin-dependent peroxide reductase, mitochondrial | P30048 | 27675 | 7.67 | 5 | -4.42 |
| PP1A Serine/threonine-protein phosphatase PP1-alpha catalytic subunit | P62136 | 38229 | 5.94 | 26 | 2.52 |
| TRXR1 Thioredoxin reductase 1, cytoplasmic | Q16881 | 71832 | 7.16 | 19 | -2.58 |
| WDR55 WD repeat-containing protein 55 | Q9H6Y2 | 42044 | 4.78 | 3 | -2.13 |
| PEO1 Twinkle protein, mitochondrial | Q96RR1 | 77619 | 9.03 | 15 | -2 |
| ARHL2 Poly(ADP-ribose) glycohydrolase ARH3 | Q9NX46 | 39264 | 4.95 | 20 | -2.64 |
| NACA Nascent polypeptide-associated complex subunit alpha | Q13765 | 23370 | 4.52 | 41 | 5.77 |
| RLA0 60S acidic ribosomal protein P0 | P05388 | 34423 | 5.71 | 49 | 13.57 |
| CHADL Chondroadherin-like protein | Q6NUI6 | 82337 | 9.2 | 1 | -2.2 |
| EF1B Elongation factor 1-beta | P24534 | 24919 | 4.5 | 53 | 3.61 |
| CLIC1 Chloride intracellular channel protein 1 | O00299 | 27248 | 5.09 | 38 | 3.81 |
| PARK7 Protein DJ-1 | Q99497 | 20050 | 6.33 | 47 | 4.86 |

*Validation of identified proteins by immunoblotting*

In order to verify the data from DIGE proteomic analysis, we measured the expression of PDIA3 and CPIN1 by western blotting analysis with the specific antibodies (Figure 9). The results demonstrated that, compared to the control group, the level of PDIA3 was increased and CPIN1 was decreased significantly with 100 μg/ml concentration of bendamustine-treated RPMI8226 cells for 2, 4, 8 or 12 h. The change patterns of the PDIA3 and CPIN1 proteins were coincident with the DIGE results. Therefore, the results of western blotting analysis verified the reliability of the proteomic analysis.

## Discussion

In this experiment, we used bendamustine at different concentrations to treat MM RPMI8226

cells with different times of exposure. According to our experimental results, bendamustine could inhibit the proliferation of MM cells in a concentration-dependent and time-dependent manner. It is accepted that bendamustine can induce cross linking reaction of both DNA chains by alkalinization to induce DNA damage which can cause apoptosis [10]. Besides, bendamustine can inhibit the activation of the checkpoints of karyokinesis and affect DNA repair. Bendamustine can also regulate the intracellular reactive oxygen species level to increase the expression of APR which is a member of the bcl-2 signal pathway family that can induce apoptosis without depending on the regulation of p53 signal pathway [11]. In conclusion, bendamustine could induce the apoptosis of MM RPMI8226 cells, but the related targeted proteins for drug action were not clearly identified.

This experiment established a model of inducing apoptosis of MM cells with bendamustine. We found the proteins the expression levels of which changed in the model before and after treatment with bendamustine by 2D-DIGE proteomics. We found 30 qualified proteins in total, 15 of which were detected with increased expression level while the other 15 were detected with decreased expression level. According to different functions, these 30 proteins could be divided into the following categories: cytoskeletal proteins, anti-oxidant proteins, molecular chaperones, zymoproteins, apoptins, ion channel proteins, etc. By studying the related literature and conducting bioinformatics analyses, among the identified proteins we chose the PDIA3 protein (with increased expression level), and the CPIN1 protein (with decreased expression level) both of which showed a close relation with apoptosis but received low attention in treating MM to prove our assumptions. These proteins might play a major role in the development of the disease and deserve our attention.

PDIA3 is a member of PDI family and is a multifunctional protein. It works as molecular chaperone during protein folding. It identifies and stabilizes the folded conformation of the polypeptide chain, and is involved in the processing of new peptide chain and correcting false folding [12,13].

PDIA3 is involved in the regulation of body's immune system, the antigen presentation and the assembling of MHC-type molecules. It combines with the immunogenicity polypeptide and presents CD8+T lymphocytes to activate T cells and then directly kills specifically the infected cells [14,15]. Mice with no PDIA3 will experience damaged antigen-polypeptide complex and its expression of antigen peptide will be influenced and then tumor cells may escape the immunosurveillance of cytotoxic T1 lymphocytes which can affect the development of tumor [16].

PDIA3 exists in the endoplasmic reticulum of cells and participates in signal transduction passage on the surface of cells. When cells are in a stress state, the expression level of PDIA3 will increase. PDIA3 regulates the STAT3-related signal pathway through the ndoplasmic reticulum cisterna. When the expression level of PDIA3 decreases, the signal transduction STAT3 will be activated. The continuous STAT3 with high activity can inhibit apoptosis and prolong the life of cells. The mechanism shows a relation with the activation of downstream target genes like Bcl-2, Bcl-xl, Mcl-1, survivin and other antiapoptotic genes, and with the inhibition of the expression of Fas protein by STAT3 combined with c-jun gene [17-19].

There are disputes about the role of PDIA3 in tumor cells. Corazzari et al. used fenretinide to induce apoptosis of neuroectodermal tumor cells and found that knockdown of PDIA3 by RNA interference in these cells increased the apoptotic response to fenretinide [20]. Pressinotti et al. interfered with the expression of PDIA3 protein in prostate cancer cells and found that the activity of caspase-3 and caspase-7 decreased significantly, indicating that PDIA3 can induce apoptosis in prostate cancer cells [21]. Those different results might be caused due to the different tumor types, pathologic processes, stages and tumor cells. We proved the proteomics conclusions in this study using the results taken by the Western blot method. Our conclusions were consistent with the report of Pressinotti et al. indicating that PDIA3 might promote apoptosis in MM cells.

In 2004, Shibayama et al. extracted the antiapoptotic molecule named CPIN1 from hematopoietic cells of mice by cloning [22]. CPIN1 participated mainly in regulating apoptosis and was an independent molecule that inhibited apoptosis. Its antiapoptotic mechanism was different from the mechanism of Bcl-2 family, the Caspase family, the IAP family and other signal transduction pathwaysmolecules. CPIN1 showed obvious inhibitory effects in multiple stages of apoptosis signal passage. The studies showed that inhibition of the expression level of CPIN1 could decrease the expression level of the antiapoptotic proteins Jak2 and Bcl-XL but increase the expression level of BAX [23]. CPIN1 also participated in regulating the RAS signal transduction passage.

CPIN1 could inhibit apoptosis and was an important effector molecule in RAS signal transduction patway passage [24].

The expression level of CPIN1 was very high in leukemia, lymphoma and other tumors of the hematopoietic system [26] and was related with the stimulation of IL-3, stem cell factor, growth factor of thrombopoietin, etc. In acute lymphocytic leukemia, acute myeloid leukemia, chronic lyphocytic leukemia and other newly diagnosed leukemias, the expression level of CPIN1 in a single karyocyte of bone marrow was higher than in a normal person [25]. According to the study of Shizusawa et al., expression of CPIN1 could be detected in 40% of diffuse large B-cell lymphoma and it was accepted that CPIN1 was a factor of unfavorable prognosis [26].

There is a correlation between CPIN1 and the multidrug resistance (MDR) mechanism of tumors. MDR is regarded as the major cause for the failure of tumor's pharmacologic treatments, although its mechanism has not been fully elucidated. It is generally accepted that MDR is related to the inhibition of apoptosis of P-glucoprotein gene, multidrug resistance protein (MRP), glutathione S transferases (GSTs), protein kinase, and topoisomerase [27]. According to the studies of MDR cells of leukemia, the expression of CPIN1 could increase the expression level of MDR-1and BCL-2 and decrease the expression level of BAX to inhibit apoptosis of tumor cells. Inhibition of CPIN1 could partially reverse the MDR mediated by CPIN1 to increase the sensitivity of leukemia cells to chemotherapy [28]. Compared with non-MDR gastric cancer cells, the expression level of CPIN1, which could lead to drug resistance by regulating P-glucoprotein and MDR-1, was much higher than that in the MDR-positive gastric cancer cells [29]. Zhang et al. indicated that CPIN1 could influence MDR without depending on the p53 signal transduction pathway [30].

Most of the relapsed or refractory MM patients show MDR [31] which limits the doctor's options for chemotherapy. Clinical researches proved that for patients with relapsed or refractory MM, administration of bendamustine alone or combined with other drugs could achieve therapeutic outcomes more than a minimum remission. Even for MM patients with bortezomib-resistant disease, bendamustine combined with bortezomib can significantly increase the remission rate, indicating that CPIN1 showes a close relationship with MDR. Decreased expression level of CPIN1 can reverse MDR and increase the sensitivity of tumor cells to anticancer agents [32]. In our study, when bendamustine was inducing apoptosis of MM cells, the expression level of CPIN1 decreased significantly. Further studies of CPIN1 could identify the relation between bendamustine and MDR to offer sound ground for clinical application.

In conclusion, the present study showed that bendamustine could induce apoptosis of MM cells. By using proteomic methods, we found that before and after bendamustine-induced the apoptosis of MM cells, 30 types of proteins showed significant changes; the expression level of PDIA3 increased while the expression level of CPIN1 decreased. The identification of these proteins offered new and important insight for studying the mechanism of bendamustine-induced apoptosis further and seeking targets for anticancer drugs.

## References


1. Mahindra A, Hideshima T, Anderson KC. Multiple myeloma:biology of the disease. Blood Rev 2010 ;24 (Suppl 1):S5-11.
2. Palumbo A, Anderson K. Multiple myeloma. N Engl J Med. 2011;364:1046-1060.
3. Cheson BD, Rummel MJ.. Bendamustine:rebirth of an old drug J Clin Oncol 2009;27:1492-1501.
4. Leoni LM, Bailey B, Reifert J et al. Bendamustine (Treanda) displays a distinct pattern of cytotoxicity and unique mechanistic features compared with other alkylating agents. Clin Cancer Res 2008;14:309-317.
5. Michael M, Bruns I, Bolke E et al. Bendamustine in patients with relapsed or refractory multiple myeloma. Eur J Med Res 2010;15:13-19.
6. Brew CT, Aronchik I, Hsu JC et al. Indole-3-carbinol activates the ATM signaling pathway independent of DNA damage to stabilize p53 and induce G1 arrest of human mammary epithelial cells. Int J Cancer 2006;118:857-868.
7. Leoni LM, Hartley JA. Mechanism of action:the unique pattern of bendamustine-induced cytotoxicity. Semin Hematol 2011;48 (Suppl 1):S12-23.
8. Dunn MJ. Proteomics reviews 2011. Proteomics 2011;11:509-512.

9. Issaq H, Veenstra T. Two-dimensional polyacrylamide gel electrophoresis (2D-PAGE):advances and perspectives. Biotechniques 2008;44:697-698.
10. Leoni LM. Bendamustine:rescue of an effective antineoplastic agent from the mid-twentieth century. Semin Hematol 2011;48 (Suppl 1):S4-11.
11. Roue G, Lopez-Guerra M, Milpied P et al. Bendamustine is effective in p53-deficient B-cell neoplasms and requires oxidative stress and caspase-independent signaling. Clin Cancer Res 2008;14:6907-6915.
12. Turano C, Gaucci E, Grillo C, Chichiarelli S. ERp57/GRP58:a protein with multiple functions. Cell Mol Biol Lett 2011;16:539-563.
13. Lumb RA, Bulleid NJ. Is protein disulfide isomerase a redox-dependent molecular chaperone. EMBO J 2002;21:6763-6770.
14. Garbi N, Hammerling G, Tanaka S. Interaction of ERp57 and tapasin in the generation of MHC class I-peptide complexes. Curr Opin Immunol 2007 ;19:99-105.
15. Panaretakis T, Joza N, Modjtahedi N et al. The co-translocation of ERp57 and calreticulin determines the immunogenicity of cell death. Cell Death Differ 2008;15:1499-1509.
16. Garbi N, Tanaka S, Momburg F, Hammerling GJ. Impaired assembly of the major histocompatibility complex class I peptide-loading complex in mice deficient in the oxidoreductase ERp57. Nat Immunol 2006;7:93-102.
17. Coe H, Jung J, Groenendyk J, Prins D, Michalak M. ERp57 modulates STAT3 signaling from the lumen of the endoplasmic reticulum. J Biol Chem 2010;285:6725-6738.
18. Bromberg J. Stat proteins and oncogenesis. J Clin Invest 2002 ;109:1139-1142.
19. Ivanov VN, Bhoumik A, Krasilnikov M et al. Cooperation between STAT3 and c-jun suppresses Fas transcription. Mol Cell 2001;7:517-528.
20. Corazzari M, Lovat PE, Armstrong JL et al. Targeting homeostatic mechanisms of endoplasmic reticulum stress to increase susceptibility of cancer cells to fenretinide-induced apoptosis:the role of stress proteins ERdj5 and ERp57. Br J Cancer 2007;96:1062-1071.
21. Pressinotti NC, Klocker H, Schafer G et al. Differential expression of apoptotic genes PDIA3 and MAP3K5 distinguishes between low- and high-risk prostate cancer. Mol Cancer 2009;8:130-149.
22. Shibayama H, Takai E, Matsumura I et al. Identification of a cytokine-induced antiapoptotic molecule anamorsin essential for definitive hematopoiesis. J Exp Med 2004;199:581-592.
23. Li X, Pan Y, Fan R et al. Adenovirus-delivered CIAPIN1 small interfering RNA inhibits HCC growth in vitro and in vivo. Carcinogenesis 2008;29:1587-1593.
24. Li X, Wu K, Fan D. CIAPIN1 as a therapeutic target in cancer. Expert Opin Ther Targets 2010;14:603-610.
25. Li B, Li QH, Lin YN, Jin WN, Pang TX. Expression of CIAPIN1 gene in BMMNC of patients with leukemia. Zhongguo Shi Yan Xue Ye Xue Za Zhi 2011;19:570-573.
26. Shizusawa T, Shibayama H, Murata S et al. The expression of anamorsin in diffuse large B cell lymphoma:possible prognostic biomarker for low IPI patients. Leuk Lymphoma 2008;49:113-121.
27. Takara K, Sakaeda T, Okumura K. An update on overcoming MDR1-mediated multidrug resistance in cancer chemotherapy. Curr Pharm Des 2006 ;12:273-286.
28. Li X, Hong L, Zhao Y et al. A new apoptosis inhibitor, CIAPIN1 (cytokine-induced apoptosis inhibitor 1) mediates multidrug resistance in leukemia cells by regulating MDR-1, Bcl-2, and Bax. Biochem Cell Biol 2007;85:741-750.
29. Li X, Fan R, Zou X et al. Reversal of multidrug resistance of gastric cancer cells by down-regulation of CIAPIN1 with CIAPIN1 siRNA. Mol Biol (Mosk) 2008;42:102-109.
30. Zhang YF, Li XH, Shi YQ et al. CIAPIN1 confers multidrug resistance through up-regulation of MDR-1 and Bcl-L in LoVo/Adr cells and is independent of p53. Oncol Rep 2011;25:1091-1098.
31. Xiao H, Xiao Q, Zhang K, Zuo X, Shrestha UK. Peversal of multidrug resistance by curcumin through FA/BRCA pathway im multiple myeloma cell line MOLP-2/R. Ann Hematol 2010;89:339-404.
32. Fenk R, Michael M, Zohren F et al. Escalation therapy with bortezomib, dexamethasone and bendamustine for patientswith relapsed or refractory multiple myeloma. Leuk Lymphoma 2007;48:2345-2351.